Hindawi
Journal of Nanomaterials
Volume 2020, Article ID 8875471, 9 pages
https://doi.org/10.1155/2020/8875471

Research Article

Synthesis of Ternary Fe_3O_4/ZnO/Chitosan Magnetic Nanoparticles via an Ultrasound-Assisted Coprecipitation Process for Antibacterial Applications

Vu Minh Thanh,[1] Nguyen Thi Huong,[1] Dao The Nam,[1] Nguyen Dinh Tien Dung,[2,3] Le Van Thu,[4] and Minh-Tri Nguyen-Le[5,6]

[1]*Institute of Chemistry and Materials, 17 Hoang Sam, Cau Giay, Hanoi, Vietnam*
[2]*Institute of Fundamental and Applied Sciences, Duy Tan University, Ho Chi Minh City 700000, Vietnam*
[3]*Faculty of Natural Science, Duy Tan University, Danang City 550000, Vietnam*
[4]*Ministry of Public Security, 80 Tran Quoc Hoan, Cau Giay, Hanoi City 100000, Vietnam*
[5]*Laboratory of Advanced Materials Chemistry, Advanced Institute of Materials Science, Ton Duc Thang University, Ho Chi Minh City 758307, Vietnam*
[6]*Faculty of Applied Sciences, Ton Duc Thang University, Ho Chi Minh City 758307, Vietnam*

Correspondence should be addressed to Minh-Tri Nguyen-Le; nguyenleminhtri@tdtu.edu.vn

Received 21 August 2020; Revised 10 November 2020; Accepted 28 November 2020; Published 16 December 2020

Academic Editor: Zheng Bao Zha

In this study, Fe_3O_4/ZnO/chitosan magnetic nanoparticles were synthesized by an ultrasound-assisted coprecipitation method. The magnetic nanoparticles were characterized by XRD, FT-IR, FESEM, and VSM techniques. The effects of ultrasonication time and content of chitosan on crystal size and lattice parameters of the nanoparticles were also studied via XRD spectra. FESEM measurements revealed that the coating consists of Fe_3O_4/ZnO nanoparticles of 15-20 nm in diameter homogeneously dispersed on the surface of chitosan substance. The VSM measurements at room temperature showed that the Fe_3O_4/ZnO/chitosan nanoparticles had superparamagnetic properties. These results indicated that ultrasonication time and chitosan content had a significant effect on the characteristics of nanoparticles. The antibacterial activities of the Fe_3O_4/ZnO/chitosan were tested against both gram-positive *Saccharomyces cerevisiae* and *Bacillus subtilis* and gram-negative *E. coli* bacteria using a disk diffusion method.

1. Introduction

Recently, iron oxide (Fe_3O_4) nanoparticles (ION) have attracted the attention of scientists all over the world due to its various applications, particularly in biomaterial engineering, such as MRI contrast agent, hyperthermia treatment, and drug delivery [1–5]. ION have been synthesized from many routes, including coprecipitation [6, 7], solvothermal method [8, 9], sol-gel method [10], microwave [11], …. Particularly, ION coated with an organic, inorganic, or polymer layer have been proved not only to prevent the aggregation of particles but also to improve the drug loading capability, solubility, biocompatibility, and selectivity of ION [12, 13]. Vu et al. successfully synthesized spherical PEG and citric acid-coated ION with a diameter of 10-15 nm and high saturation magnetization value of 70.52 emu/g [14].

Chitosan, a nontoxic biopolymer structured from glucosamines, has been used as a potential surface-protecting layer for ION in recent years. In addition to its biocompatibility, biodegradability, and adsorption ability, chitosan with amine groups has also shown the ability to control drug release, improve drug diffusion, and enhance drug permeation [15]. Moreover, chitosan has emerged as an antibacterial and antiviral agent due to its positive charge which helps it adhere to negatively charged surfaces and interact with polyanions to form a gel structure [16]. Like chitosan, utilization of ZnO nanoparticles in the controlled drug release and tumour cell destruction has been also reported [17]. ZnO is an n-type

semiconductor with a wide band gap (3.1-3.3 eV) and high activated energy (60 meV) at room temperature, which has led to a variety of unique optical and thermal properties of ZnO nanoparticles [18, 19]. The combination of chitosan and inorganic nanoparticles like ZnO would form antibacterial materials with multifunctional properties [20]. Yuan et al. reported the synthesis of chitosan-ZnO by a chemical degradation method for targeted drug delivery [21]. The chitosan-ZnO complex was proved to be a more effective antibacterial agent than chitosan [22, 23]. Moreover, the combination of ZnO and other polymers like chitosan can prevent the intrinsic aggregation of ZnO nanoparticles due to their small size [24].

A nonconventional ultrasonic method has been known as an effective and environmentally friendly method for chemical modifications of polymers which have a variety of applications. For instance, Barreto et al. reported the fabrication of a chitosan/ZnO complex under high-intensity ultrasonic radiation. The hybrid showed the highest antibacterial activity against *Staphylococcus aureus* (gram-positive) and *Escherichia coli* (gram-negative) bacteria [25]. The ultrasonic-assisted method also exhibited its effectiveness in the preparation of ternary chitosan/ZnO/TiO_2 nanocomposite for crystal violet (CV) dye adsorption reported by Bhanvasea et al. [26]. Similarly, the work performed by Vardikar et al. revealed that the kaolin-chitosan-TiO_2 ternary nanocomposites synthesized by a sonochemical route had many advantages for dye adsorption over those prepared by a conventional method [27]. To the best of our knowledge, there is a lack of reports on the synthesis of ternary Fe_3O_4/ZnO/chitosan nanoparticles via a coprecipitation ultrasonication method for antibacterial and antifungal application.

Therefore, in this research, we synthesized Fe_3O_4/ZnO/chitosan nanoparticles using a coprecipitation-ultrasonication method. ZnO nanoparticles were synthesized using rambutan peel extraction and zinc nitrate hexahydrate. The effects of chitosan concentration, magnetic properties, and antibacterial activity were also investigated.

2. Materials and Methods

2.1. Materials. Ferric chloride hexahydrate ($FeCl_3{\cdot}6H_2O$), ferrous chloride tetrahydrate ($FeCl_2{\cdot}4H_2O$), zinc nitrate hexahydrate ($Zn(NO_3)_2{\cdot}6H_2O$), and ethanol were purchased from Merck. Low molecular weight chitosan (CS: 100-200 mPa·s) was purchased from Aladin, China. The PEG polymers (PEG-6000) and NH_3 solution were obtained from Macklin-China, India. Rambutan (Nephelium lappaceum L.) peel was collected in Vietnam. Deionized water was used for the preparation of all aqueous solutions.

2.2. Preparation of PEG-Coated Fe_3O_4 and ZnO Nanoparticles. Firstly, $FeCl_3{\cdot}6H_2O$ and $FeCl_2{\cdot}4H_2O$ with a ratio of 2 : 1 were mixed together with 100 ml of deionized water. The reaction mixture was then placed on a sonicator (Sonics & Materials—VCX500; 500 W, 20 kHz). 25-28% NH_3 solution was added dropwise to the solution to obtain black precipitated Fe_3O_4 nanoparticles using a syringe pump with a flow rate of 50 ml/h. The obtained solid was washed with ethanol twice then with distilled water several times until reaching the neutral pH. The product was dried in an oven at 65°C for 24 h. The PEG-coated Fe_3O_4 nanoparticles (PEG-Fe_3O_4) were prepared by adding Fe_3O_4 into PEG solution at room temperature under ultrasonication for 6 h.

ZnO nanoparticles were prepared according to a previous rambutan (*Nephelium lappaceum L.*) peel extraction method [24, 28]. Rambutan peels were washed with water, cut into small pieces, and subsequently placed in a circulating oven at 60°C until completely dried. 3 g of the dried rambutan peels was boiled with a mixture of ethanol and distilled water (1 : 2, *v*/*v*) for 30 min during the extraction. The extract was passed through a Whatman No.1 filter and stored in a refrigerator for further use. 0.1 M zinc nitrate hexahydrate was prepared in 50 ml deionized water, and then, 50 ml of rambutan peel extract (Vietnam) was slowly added dropwise into the solution under magnetic stirring at room temperature, and the solution was sonicated for 1 h in an ultrasonic bath (500 W, 20 kHz) to obtain a zinc-ellagate complex. The zinc-ellagate complex was collected by centrifugation at 7000 rpm for 20 min. Then, the solid was washed with distilled water, dried in an oven at 40°C for 8 h, and calcinated in a muffle furnace at 450°C to obtain ZnO nanoparticles.

2.3. Preparation of Fe_3O_4/ZnO/Chitosan. For the synthesis of Fe_3O_4/ZnO/chitosan, PEG-Fe_3O_4 and ZnO (1 : 1, *w*/*w*) were firstly dissolved in 100 ml of deionized water. The solution was mixed homogeneously using a magnetic stirrer at temperature for 10 min. Then, the reaction mixture was placed in a sonicator (VCX500; 500 W, 20 kHz) for 30 min. Meanwhile, chitosan was added to 30 ml of 1% aqueous acetic acid and agitated for 30 min to obtain a chitosan solution. The two obtained solutions were mixed together to form a white emulsion. In the preparation of Fe_3O_4/ZnO/chitosan magnetic nanoparticles, the emulsion was dropped into the mixture homogenous (PEG-Fe_3O_4/ZnO) using a sonicator (VCX500; 500 W, 20 kHz) for 30 min. The Fe_3O_4/ZnO/chitosan was separated under an external magnetic field and washed two times with deionized water, then finally dried in a vacuum oven at 60°C. The effect of different mass ratios of CS and PEG-Fe_3O_4/ZnO on the magnetic properties of Fe_3O_4 was investigated by varying different mass percentages of chitosan (5%, 10%, 20%, and 30%). Fe_3O_4/ZnO/chitosan samples with different amounts of chitosan were denoted as Fe_3O_4/ZnO/chitosan 5%, Fe_3O_4/ZnO/chitosan 10%, Fe_3O_4/ZnO/chitosan 20%, and Fe_3O_4/ZnO/chitosan 30%. Figure 1 shows the schematic of the preparation of Fe_3O_4/ZnO/chitosan magnetic nanoparticles.

2.4. Characterizations. X-ray diffraction patterns were recorded on a P'Pret Pro-PANalytical X-ray diffractometer operated at 1.8 kW (40 mA/45 kV) using CuKα ($\lambda = 1.5406$ Å) radiation. FT-IR spectra were recorded on a Bruker FT-IR spectrometer using the KBr pellet method. FESEM was carried out using a Hitachi S-4800 microscope. To prepare FESEM samples, a small amount of the solid sample was dispersed in ethanol and small drops of the solution were placed on an aluminum grid. The grid was dried for 1-2 h in a vacuum oven at 40°C prior to the FESEM measurement.

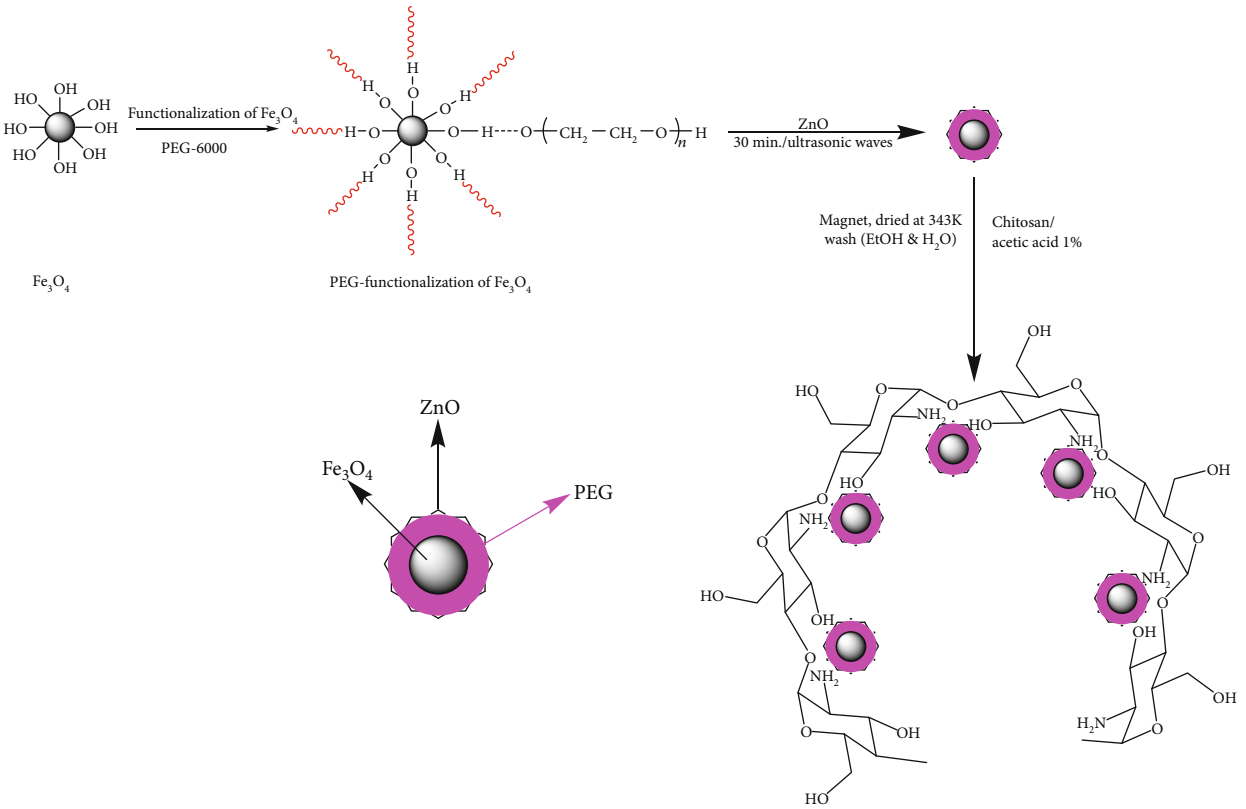

Figure 1: The schematic of the preparation of Fe_3O_4/ZnO/chitosan magnetic nanoparticles.

Magnetic measurements of the solid samples were performed at room temperature (25°C) using a Magnet B-10 Vibrating Sample Magnetometer (VSM). The surface morphology of the sample was imaged by transmission electron microscopy (TEM-JEM1010). TEM images were acquired at an operating voltage of 80 kV. The size and ζ-potential of the sample were recorded on a Malvern Zetasizer Nano Z instrument (Malvern Instruments, Ltd., UK). Nanoparticle dispersions were prepared in D.I. water at 37°C with a concentration of 1 mg/ml.

2.5. Antibacterial Activity Testing. The antibacterial activity of Fe_3O_4/ZnO/chitosan was tested against both gram-positive *Bacillus subtilis* and *Saccharomyces cerevisiae* and gram-negative (*E. coli* ATCC 11632) bacteria using a disk diffusion method. The enrichment medium containing meat extract, yeast extract, peptone, glucose, and some mineral salts was used for microbiological cultivation. For comparison, chitosan and positive control disks were also involved in the test. The antibacterial and antifungal activities were evaluated by measuring the zone of inhibition against the tested organisms.

The antibacterial activity experiments were conducted as follows: First, the petri dishes containing appropriate media for the growth of bacteria were prepared. Then, two aforementioned testing materials were sprinkled on these dishes to be evaluated by their mortality in the cultured medium, followed by the inoculation of the suspended solutions

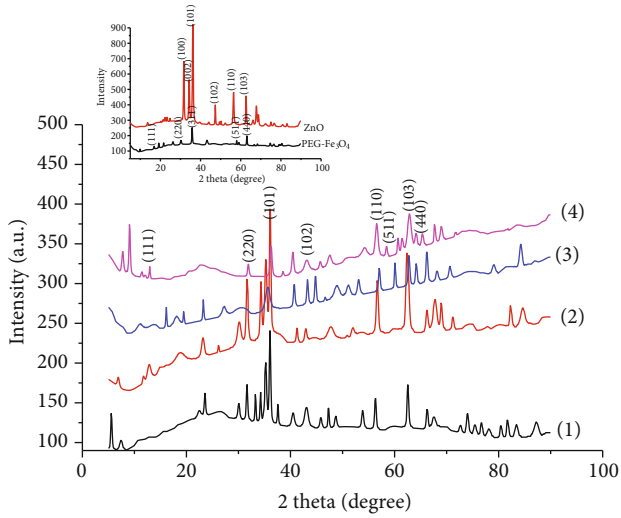

(1) Fe_3O_4/ZnO/CS 5%
(2) Fe_3O_4/ZnO/CS 10%
(3) Fe_3O_4/ZnO/CS 20%
(4) Fe_3O_4/ZnO/CS 30%

Figure 2: XRD patterns of PEG-Fe_3O_4, ZnO, and Fe_3O_4/ZnO/chitosan samples.

obtained from each of the three bacterial strains on the petri dishes with appropriate enrichment media.

The control sample was prepared as follows: the testing materials were sprinkled on petri dishes with the inoculated

Table 1: Effects of CS content upon crystallite size and lattice parameters of PEG-Fe_3O_4/ZnO/CS magnetic nanoparticles.

Samples		ZnO	PEG-Fe_3O_4	Fe_3O_4/ZnO/CS			
				5%	10%	20%	30%
Crystallite size[a] (nm)	ZnO	20.7465	—	27.9867	27.9894	28.3849	27.6781
	Fe_3O_4	—	20.9798	20.9408	20.7469	18.386	21.0030
Lattice parameter[b] (Å)	ZnO	$a = b = 3.2427$ $c = 5.1948$ $\alpha = \beta = 90^\circ$ $\gamma = 120^\circ$	—	$a = b = 3.5222$ $c = 5.2363$	$a = b = 3.5190$ $c = 5.2257$	$a = b = 3.1334$ $c = 4.1805$	$a = b = 3.5078$ $c = 5.6112$
	Fe_3O_4	—	$a = b = c = 8.3232$ $\alpha = \beta = \gamma = 90^\circ$	$a = b = c = 8.4505$	$a = b = c = 8.4422$	$a = b = c = 8.3651$	$a = b = c = 8.3637$

[a]Obtained from Debye-Scherrer equation (1). [b]Obtained from (2), (3), and (4).

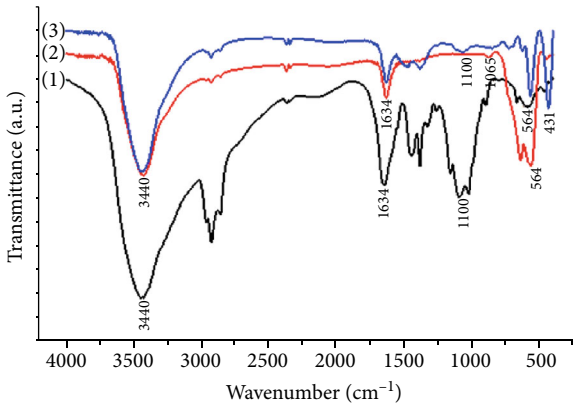

(1) CS
(2) PEG-Fe_3O_4/ZnO
(3) PEG-Fe_3O_4/ZnO/CS

Figure 3: FT-IR spectra of (1) CS, (2) PEG-Fe_3O_4/ZnO, and (3) PEG-Fe_3O_4/ZnO/CS.

suspensions of microorganisms. Certain amounts of the testing materials were placed in the Eppendorf tubes prior to the aspiration of the bacterial suspensions into the respective tubes. All samples were then well shaken for 20 min. Afterwards, a small quantity of each sample was aspirated and placed on petri dishes containing appropriate media for evaluating the antibacterial activity of the testing materials. All samples were incubated in a container at 37°C for 24 to 72 h.

3. Results and Discussion

3.1. Structural and Morphological Studies. During the preparation of PEG-coated Fe_3O_4 nanoparticles, ZnO nanoparticles, and Fe_3O_4/ZnO/chitosan magnetic nanoparticles, the color of the reaction mixtures changed several times due to the formation of different substances. Once the ammonia solution was added to the reaction solutions, it produced OH^- anions reacting with Fe^{2+} and Fe^{3+} cations to form Fe_3O_4 nanoparticles. The addition of PEG to the reaction mixture resulted in the formation of PEG-coated Fe_3O_4 nanoparticles. This happened due to the interaction between H atoms in O-H groups of PEG and O atoms on the surface of Fe_3O_4 nanoparticles [29].

ZnO nanoparticles were synthesized using rambutan peel extract which contains phenolic antioxidants. A zinc-ellagate complex was formed after 1 h sonication of the solution containing rambutan peel extract and zinc nitrate hexahydrate. It was ascribed to the formation of bonding between hydroxyl groups of phenolic compounds and the zinc metal as a metal phenolate complex by the chelating effect in which the ester oxygen atoms and phenolic hydroxyl groups of phenolic compounds form p-track conjugation effect [28]. The decomposition of the zinc-ellagate complex at 450°C led to formation of ZnO nanoparticles [28]. Then, ZnO nanoparticles were attached to the PEG-Fe_3O_4 via hydrogen bondings between PEG-Fe_3O_4 and ZnO and externally coated by the CS as shown in Figure 1. The incorporation of ZnO into the material system was aimed at creating a composite of the chitosan-based system to increase the antibacterial ability against gram-negative bacteria. The products were further characterized by XRD, FT-IR, and VSM. Figure 2 describes the XRD patterns of the bare PEG-Fe_3O_4, ZnO, and Fe_3O_4/ZnO/chitosan samples.

The XRD peak positions and their relative intensities in all XRD patterns were well matched with the standard cards of Fe_3O_4 (ICSD code: 084611) and ZnO (ICSD code: 065122). The characteristic peaks of Fe_3O_4 located at 2θ values of 30.0°, 35.4°, 57.2°, and 62.6° revealed a cubic spinel structure of Fe_3O_4 nanoparticles [27]. Meanwhile, the characteristic peaks of ZnO could be observed at 2θ values of 31.76°, 34.28°, 36.12°, 47.30°, 56.37°, and 68.77°, which are indicative of a hexagonal structure [24, 28]. The XRD pattern of Fe_3O_4/ZnO/chitosan samples with different CS contents showed all of the characteristic peaks of both Fe_3O_4 and ZnO crystals. Interestingly, the XRD patterns of (2), (3), and (4) exhibited broad diffraction peaks at $2\theta = 19.65^\circ$ and 23.34°, which are typical fingerprints of CS with an amorphous nature [30, 31].

*The Debye-Scherrer equation (Equation (1)) was used to calculate crystallite size:

$$d = \frac{k\lambda}{\beta \cos\theta}, \quad (1)$$

where d is the mean crystallite size (nm), k is the crystallite shape constant (approximately taken as 0.89), λ is the X-

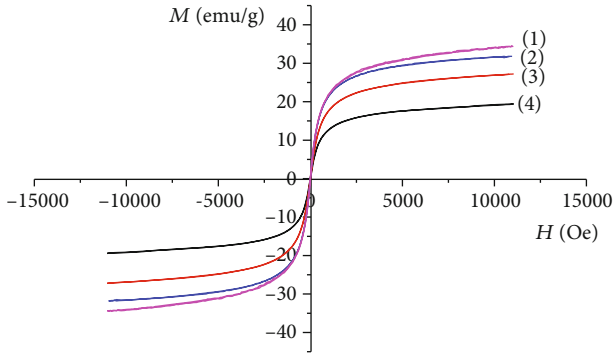

(1) Fe_3O_4/ZnO/CS 5%
(2) Fe_3O_4/ZnO/CS 10%
(3) Fe_3O_4/ZnO/CS 20%
(4) Fe_3O_4/ZnO/CS 30%

Figure 4: M-H curves of Fe_3O_4/ZnO/chitosan samples.

ray wavelength (nm), β is the full width at half maximum height of the X-ray diffraction peak, and θ is the Bragg angle (degree).

*The distance between atomic layers of a crystal was calculated by Bragg's law:

$$n\lambda = 2d_{hkl} \sin \theta_{hkl}, \quad (2)$$

where n is any integer; d_{hkl} is the distance between atomic layers of a crystal (Å); θ_{hkl} is the incident angle, the angle between the incident rays, and the scatter plane (degree); and λ is the wavelength of the incident X-ray beam (nm).

Based on the function of Miller Indices and lattice parameters, we can determine the formula for interplanar spacing of Fe_3O_4 cubic crystals with $a = b = c$; $\alpha = \beta = \gamma = 90^\circ$ as follows:

$$\frac{1}{d_{hkl}^2} = \frac{h^2 + k^2 + l^2}{a^2}. \quad (3)$$

Meanwhile, the formula for interplanar spacing of ZnO hexagonal crystals with $a = b, c$; $\alpha = \beta = 90^\circ, \gamma = 120^\circ$ can be determined as follows:

$$\frac{1}{d_{hkl}^2} = \frac{4}{3}\left(\frac{h^2 + hk + k^2}{a^2}\right) + \frac{l^2}{c^2}, \quad (4)$$

where h, k, l is Miller Indices, d_{hkl} is interplanar spacing (nm), and a, b, c are lattice parameters.

Effects of CS content on the crystallite size and lattice parameters of PEG-Fe_3O_4/ZnO/CS nanoparticle are shown in Table 1. The crystallite size of the Fe_3O_4 phase in Fe_3O_4/ZnO/CS nanoparticles and its lattice parameters were not different from those in the PEG-Fe_3O_4 substrate, while the crystallite size of the ZnO phase in Fe_3O_4/ZnO/CS nanoparticles increased as compared to the ZnO containing substances. This is due to the fact that Fe_3O_4 crystals were coated with PEG and were less affected than ZnO crystals during Fe_3O_4/ZnO/chitosan nanocomposite synthesis.

Figure 3 describes the FT-IR curves of CS and PEG-Fe_3O_4/ZnO and PEG-Fe_3O_4/ZnO/CS samples.

The FT-IR spectra of all samples showed absorption peaks at around 3440 cm^{-1} and 1634 cm^{-1} which are related to the OH groups or NH_2 groups. Additionally, the CS (1) and PEG-Fe_3O_4/ZnO/CS (3) spectra exhibited the characteristic IR peaks of β(1-4) glycosidic bands in the polysaccharide unit at 1110 cm^{-1} and 1065 cm^{-1} indicated the stretching vibration of C-O-C in glucose circle [28]. However, these peaks were absent from PEG-Fe_3O_4/ZnO (2) spectra. Instead, it showed strong absorption in the fingerprint range at 564 cm^{-1}, indicating the presence of Fe-O bond in the Fe_3O_4-PEG sample [13]. The Fe-O-C bond interaction identified by the absorption around 1100 cm^{-1} indicated that Fe_3O_4 was successfully coated with PEG [30]. The FT-IR spectra of PEG-Fe_3O_4/ZnO/CS (3) showed absorption peaks at around 431 cm^{-1} which are the stretching vibrations of N-Zn and Zn-O [32]. As compared to the spectra of (2), the bands at 1100 cm^{-1} and 564 cm^{-1} in the (3) sample have a reduced intensity as a result of the external coating of the CS gel on the PEG-Fe_3O_4/ZnO core, which is shown in Figure 1.

Magnetic measurements were conducted using a vibrating sample magnetometer (Figure 4). Magnetization curves were recorded at room temperature, and parameters such as coercive field (Hc) and initial susceptibility (χi) were obtained. The saturation magnetization (Ms) was obtained by extrapolation to the infinite field of the experimental data obtained in the high-field range where the magnetization varied linearly with the inverse of the applied field. Saturation magnetization values were normalized by taking into account the percentage of CS contained in the samples.

The saturation magnetization of bare Fe_3O_4 nanoparticles was reported as 68.9 emu/g [4]. After coating Fe_3O_4 with PEG, the saturation magnetization of PEG-Fe_3O_4 was determined as 65.71 emu/g [2]. The saturation magnetization of Fe_3O_4/ZnO/CS nanocomposite decreased from 20% to 75% as compared to the PEG-Fe_3O_4 substrate depending on the CS content in the samples. The saturation magnetization of PEG-Fe_3O_4/ZnO/CS 5%, PEG-Fe_3O_4/ZnO/CS 10%, PEG-Fe_3O_4/ZnO/CS 20%, and PEG-Fe_3O_4/ZnO/CS 30% was 34.51, 31.69, 27.12, and 19.43 emu/g, respectively.

FESEM, TEM images, and size distribution in Figure 5 showed that PEG-Fe_3O_4/ZnO nanoparticles after the surface modification with CS had a softer surface and more uniform particle size distribution than the bare Fe_3O_4 and PEG-Fe_3O_4/ZnO samples. The obtained PEG-Fe_3O_4/ZnO material is under composite form of Fe_3O_4 and ZnO; both PEG-Fe_3O_4/ZnO and Fe_3O_4/ZnO/chitosan samples exhibited the sizes of nano-Fe_3O_4 and ZnO particles in the range of 13-20 nm. Particle size distribution by the DLS method showed that the material system had an average size of 354 nm. The size measured by the DLS method was larger than that by TEM because DLS determined the hydrodynamic diameter of particles including polymer cover (PEG) along with the swelling of chitosan in water. Similar to the SEM measurement, the TEM showed that the chitosan film encased Fe_3O_4/ZnO nanoparticles.

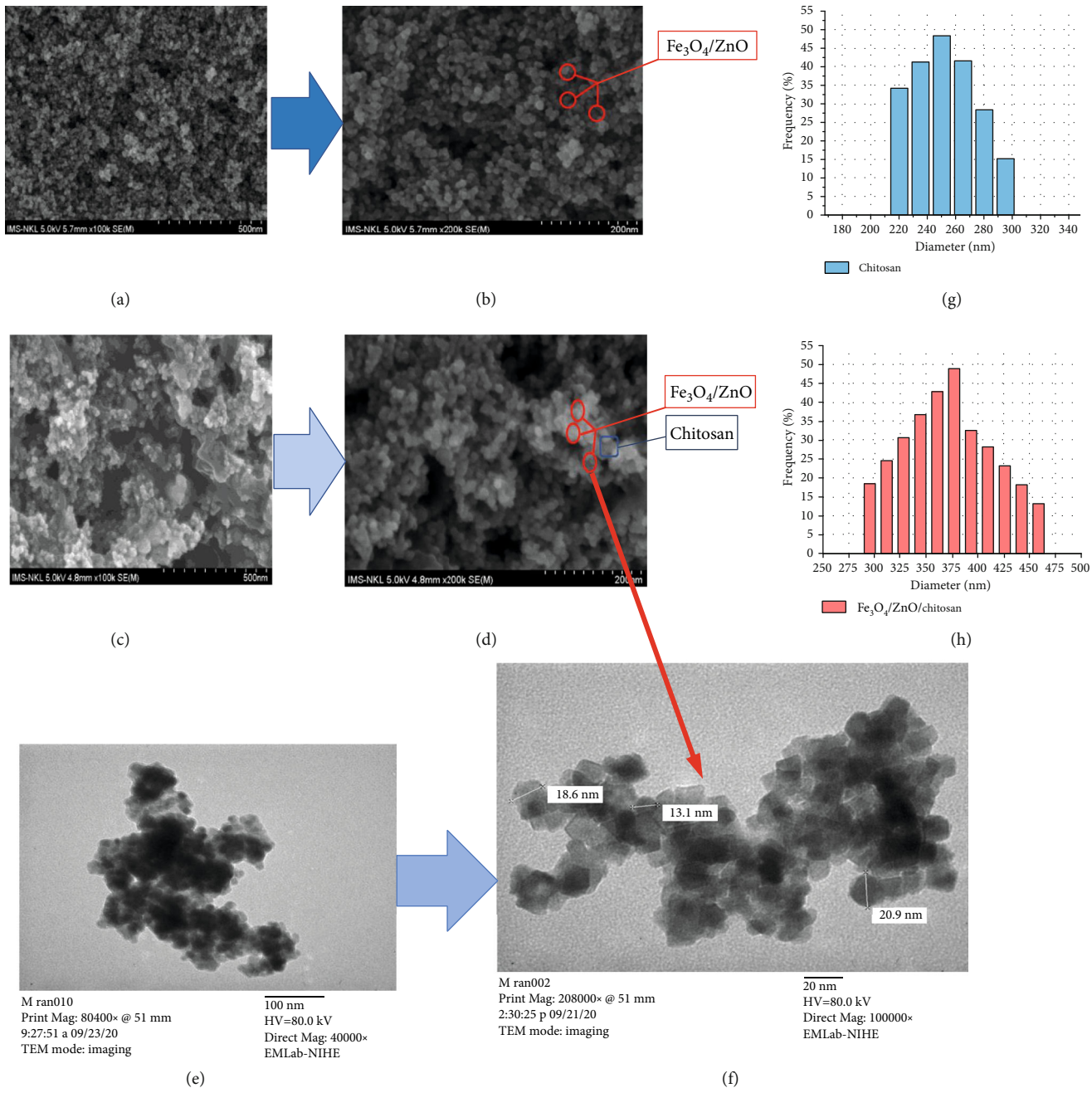

Figure 5: FESEM images of (a, b) PEG-Fe_3O_4/ZnO and (c, d) Fe_3O_4/ZnO/CS nanocomposites. (e, f) TEM images of Fe_3O_4/ZnO/CS nanocomposites. Size distribution of chitosan (g) and Fe_3O_4/ZnO/CS nanocomposites (h) measured by DLS.

The results showed that the zeta potential values of the chitosan and Fe_3O_4/ZnO/chitosan nanoparticles were 8.13 mV and 4.56 mV, respectively. The surface charges of the matrix material and the composite were positive due to the presence of the NH_3^+ ions in the chitosan groups. When the PEG-Fe_3O_4/ZnO composite system was incorporated with chitosan, the interaction of the OH groups on the composite surface and the NH_3^+ groups of chitosan would reduce the zeta potential of the Fe_3O_4/ZnO/chitosan nanoparticle system. The change of the zeta potential of the materials would result in a change in the interaction between the material and the cell of gram-positive and gram-negative bacteria.

3.2. Antibacterial Activity. The survivability of microorganisms (fungi and bacteria) after contacting with testing materials is shown in Figure 6. It could be clearly observed that all two petri dishes showed no signs of bacterial or fungal growth on the nutrient medium surfaces when certain amounts of testing samples were sprinkled on the nutrient media and incubated in suitable conditions for 72 h (Figures 6(c)–6(h)). The results indicated that Fe_3O_4/ZnO/-chitosan reached its best capability to inhibit the growth of *Bacillus subtilis*, *Saccharomyces cerevisiae*, and *E.coli*. Also, clear zones (nonbacterial zones) were established at the sprinkled points of Fe_3O_4/ZnO/chitosan on the *Bacillus*

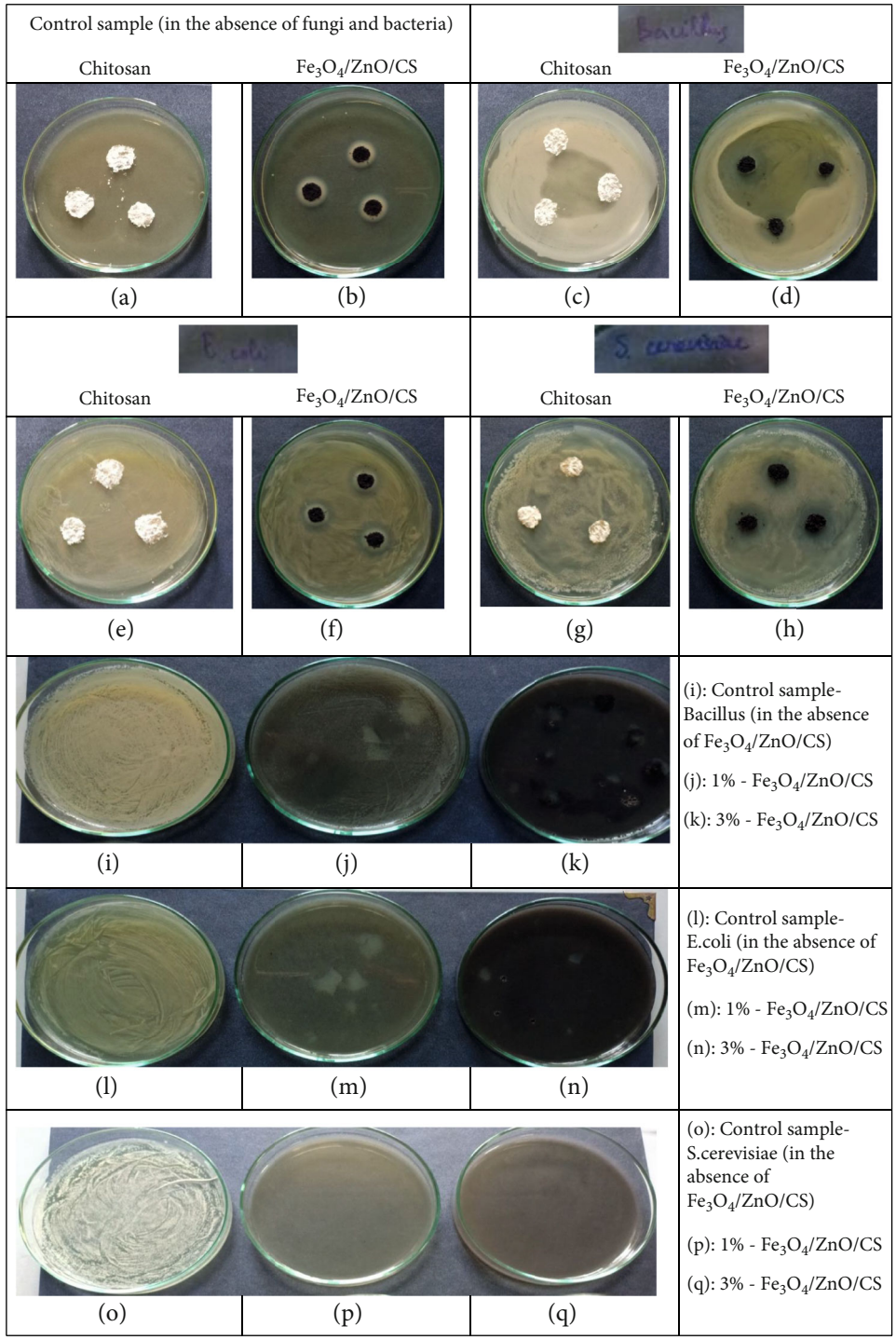

FIGURE 6: Antibacterial and antifungal of chitosan and Fe3O4/ZnO/chitosan sprinkled on the nutrient media (c–h); Antibacterial and antifungal of Fe3O4/ZnO/chitosan evenly spread on the nutrient media at different concentrations (j, k; m, n; p, q). Respective control samples (a, b; i, l, o).

subtilis and *Saccharomyces cerevisiae* inoculated petri dishes. Moreover, the suspensions were evenly spread on the controlled dishes without testing materials. Growth of microorganisms to a smooth and thick layer on the dish surfaces was observed (Figures 6(i), 6(l), and 6(o)). However, in the presence of Fe_3O_4/ZnO/chitosan, the cellular density of *Bacillus*, *Saccharomyces cerevisiae*, and *E. coli* was significantly decreased. Therefore, it can be concluded that Fe_3O_4/ZnO/chitosan had the ability to inhibit the *Bacillus*, *S. cerevisiae*, and *E. coli* strains.

4. Conclusions

We have successfully prepared Fe_3O_4/ZnO/chitosan magnetic nanoparticles using the ultrasound-assisted coprecipitation method. Based on the XRD data of the samples

obtained with the variation of CS content, it can be concluded that the crystallite size of Fe_3O_4 nanoparticles and their lattice parameters were almost no different from the PEG-Fe_3O_4 sample while the crystal size of ZnO increased as compared to the ZnO substance sample. The modified surface of nanoparticles resulted in the softening of magnetization. The results from studying the survivability when in contact with testing materials proved the ability of Fe_3O_4/ZnO/chitosan to inhibit the growth of a large number of microorganisms. Fe_3O_4/ZnO/chitosan possessed the ability to eliminate not only bacterial cells but also fungal (mold) cells on the material surfaces and worked well with the bacterial Bacillus subtilis strains.

Data Availability

The data used to support the findings of this study are included within the article.

Conflicts of Interest

The authors declare that there is no conflict of interest regarding the publication of this paper.

Acknowledgments

This research is funded by the Vietnam National Foundation for Science and Technology Development (NAFOSTED) under grant number 104.06-2018.320.

References

[1] D. Frascione, C. Diwoky, G. Almer et al., "Ultrasmall superparamagnetic iron oxide (USPIO)-based liposomes as magnetic resonance imaging probes," *International Journal of Nanomedicine*, vol. 7, pp. 2349–2359, 2012.

[2] T. T. Hoang Thi, D. H. Nguyen Tran, L. G. Bach et al., "Functional magnetic core-shell system-based iron oxide nanoparticle coated with biocompatible copolymer for anticancer drug delivery," *Pharmaceutics*, vol. 11, no. 3, p. 120, 2019.

[3] T. N. Le Thi, T. H. Nguyen, D. Q. Hoang, T. V. Tran, N. T. Nguyen, and D. H. Nguyen, "Development of new magnetic nanoparticles: oligochitosan obtained by γ-rays and –coated Fe3O4 nanoparticles," *Applied Surface Science*, vol. 422, pp. 863–868, 2017.

[4] D. Q. Hoang, T. V. Tran, N. Q. Tran et al., "Functionalization of Fe_3O_4 nanoparticles with biodegradable chitosan-grafted-mPEG for paclitaxel delivery," *Green Processing and Synthesis*, vol. 5, no. 5, 2016.

[5] H. D. Nguyen, T. D. Nguyen, D. H. Nguyen, and P. T. Nguyen, "Magnetic properties of Cr doped Fe3O4porous nanoparticles prepared through a co-precipitation method using surfactant," *Advances in Natural Sciences: Nanoscience and Nanotechnology*, vol. 5, no. 3, article 035017, 2014.

[6] T. H. Nguyen, N. T. T. Le, T. D. Cong et al., "Effect of ultrasonication time and peg content on the crystallite size and lattice parameter of polyethylene glycol (peg)-coated Fe_3O_4 nanoparticles synthesized by a ultrasound assiste co-precipitation process," *Vietnam Journal of Chemistry*, vol. 57, pp. 340–346, 2019.

[7] M. Abbasian, F. Mahmoodzadeh, A. Khalili, and R. Salehi, "Chemotherapy of breast cancer cells using novel pH-responsivecellulose-based nanocomposites," *Advanced Pharmaceutical Bulletin*, vol. 9, no. 1, pp. 122–131, 2019.

[8] S. Sun and H. Zeng, "Size-controlled synthesis of magnetite nanoparticles," *Journal of the American Chemical Society*, vol. 124, no. 28, pp. 8204-8205, 2002.

[9] T. K. O. Vuong, D. L. Tran, T. L. le et al., "Synthesis of high-magnetization and monodisperse Fe_3O_4 nanoparticles via thermal decomposition," *Materials Chemistry and Physics*, vol. 163, pp. 537–544, 2015.

[10] M. Liu, X. Sun, Z. Liao et al., "Zinc oxide end-capped Fe_3O_4@mSiO_2core-shell nanocarriers as targeted and responsive drug delivery system for chemo-/ions synergistic therapeutics," *Drug Delivery*, vol. 26, no. 1, pp. 732–743, 2019.

[11] K. Zhang, X. Zhang, X. Zhao et al., "Polypyrrole coated Fe3O4 nanoparticles decorated carbon nanotubes nanocomposites and the microwave absorption properties," *Journal of Materials Science: Materials in Electronics*, vol. 30, no. 18, pp. 17333–17341, 2019.

[12] L. Li, K. Y. Mak, C. W. Leung et al., "Effect of synthesis conditions on the properties of citric-acid coated iron oxide nanoparticles," *Microelectronic Engineering*, vol. 110, pp. 329–334, 2013.

[13] Z. Li, L. Wei, M. Gao, and H. Lei, "One-pot reaction to synthesize biocompatible magnetite nanoparticles," *Advanced Materials*, vol. 17, no. 8, pp. 1001–1005, 2005.

[14] M. T. Vu, T. N. Dao, T. P. Pham et al., "Modified iron oxide nanoparticles with polyethylene glycol and citric acid for biomedical applications," *Vietnam Journal of Chemistry*, vol. 57, 2019.

[15] A. Ali and S. Ahmed, "A review on chitosan and its nanocomposites in drug delivery," *International Journal of Biological Macromolecules*, vol. 109, pp. 273–286, 2018.

[16] W. Tachaboonyakiat, "Antimicrobial applications of chitosan," in *Chitosan Based Biomaterials Volume 2*, vol. 2, pp. 245–274, 2017.

[17] H. Qiu, B. Cui, G. Li et al., "Novel Fe_3O_4@ZnO@mSiO_2nanocarrier for targeted drug delivery and controllable release with microwave irradiation," *The Journal of Physical Chemistry C*, vol. 118, no. 27, pp. 14929–14937, 2014.

[18] M. Roeinfard and A. Bahari, "Nanostructural characterization of the Fe_3O_4/ZnO magnetic nanocomposite as an application in medicine," *Journal of Superconductivity and Novel Magnetism*, vol. 30, no. 12, pp. 3541–3548, 2017.

[19] Ü. Özgür, Y. I. Alivov, C. Liu et al., "A comprehensive review of ZnO materials and devices," *Journal of Applied Physics*, vol. 98, no. 4, p. 041301, 2005.

[20] S. P. Singh, "Multifunctional magnetic quantum dots for cancer theranostics," *Journal of Biomedical Nanotechnology*, vol. 7, no. 1, pp. 95–97, 2011.

[21] Q. Yuan, S. Hein, and R. D. K. Misra, "New generation of chitosan-encapsulated ZnO quantum dots loaded with drug: synthesis, characterization and in vitro drug delivery response," *Acta Biomaterialia*, vol. 6, no. 7, pp. 2732–2739, 2010.

[22] I. Perelshtein, E. Ruderman, N. Perkas et al., "Chitosan and chitosan-ZnO-based complex nanoparticles: formation, characterization, and antibacterial activity," *Journal of Materials Chemistry B*, vol. 1, no. 14, pp. 1968–1976, 2013.

[23] P. Mujeeb Rahman, V. M. Abdul Mujeeb, K. Muraleedharan, and S. K. Thomas, "Chitosan/nano ZnO composite films:

enhanced mechanical, antimicrobial and dielectric properties," *Arabian Journal of Chemistry*, vol. 11, no. 1, pp. 120–127, 2018.

[24] P. E. Ochieng, E. Iwuoha, I. Michira et al., "Green route synthesis and characterization of ZnO nano nanoparticles using spathodea campanulate," *International Journal of BioChemiPhysics*, vol. 23, pp. 53–60, 2015.

[25] M. S. R. Barreto, C. T. Andrade, E. G. Azero, V. M. F. Paschoalin, and E. M. del Aguila, "Production of chitosan/zinc oxide complex by ultrasonic treatment with antibacterial activity," *Journal of Bacteriology & Parasitology*, vol. 8, no. 5, 2017.

[26] B. A. Bhanvase, A. Veer, S. R. Shirsath, and S. H. Sonawane, "Ultrasound assisted preparation, characterization and adsorption study of ternary chitosan-ZnO-TiO_2 nanocomposite: advantage over conventional method," *Ultrasonics Sonochemistry*, vol. 52, pp. 120–130, 2019.

[27] H. S. Vardikar, B. A. Bhanvase, A. P. Rathod, and S. H. Sonawane, "Sonochemical synthesis, characterization and sorption study of kaolin-chitosan-TiO2 ternary nanocomposite: advantage over conventional method," *Materials Chemistry and Physics*, vol. 217, pp. 457–467, 2018.

[28] R. Yuvakkumar, J. Suresh, A. J. Nathanael, M. Sundrarajan, and S. I. Hong, "Novel green synthetic strategy to prepare ZnO nanocrystals using rambutan (Nephelium lappaceum L.) peel extract and its antibacterial applications," *Materials Science and Engineering C*, vol. 41, pp. 17–27, 2014.

[29] S. Bagheri and N. M. Julkapli, "Modified iron oxide nanomaterials: functionalization and application," *Journal of Magnetism and Magnetic Materials*, vol. 416, pp. 117–133, 2016.

[30] D. S. Vicentini Jr., A. Smania, and M. C. M. Laranjeira, "Chitosan/poly (vinyl alcohol) films containing ZnO nanoparticles and plasticizers," *Materials Science and Engineering C*, vol. 30, no. 4, pp. 503–508, 2010.

[31] M. Anand, P. Sathyapriya, M. Maruthupandy, and A. Hameedha Beevi, "Synthesis of chitosan nanoparticles by TPP and their potential mosquito larvicidal application," *Frontiers in Laboratory Medicine*, vol. 2, no. 2, pp. 72–78, 2018.

[32] L. G. Tang, D. N. S. Hon, and S. Hon, "Chelation of chitosan derivatives with zinc ions. II. Association complexes of Zn^{2+} ontoO,N-carboxymethyl chitosan," *Journal of Applied Polymer Science*, vol. 79, no. 8, pp. 1476–1485, 2001.